Low Pressure Gaseous Detector for Particle Dark Matter

K. N. Buckland, M. J. Lehner, G. E. Masek, and M. Mojaver
Physics Department, University of California at San Diego, La Jolla, California 92093
(Received 22 March 1994; revised manuscript received 29 June 1994)

The results of recent testing of a prototype detector to search for weakly interacting massive particles in the galactic halo are presented. The detector is an optically imaged, low pressure time projection chamber. This technique offers significant advantages for the detection of dark matter in that it measures both the energy and direction of the nuclear recoil. Using neutron and x-ray sources we also demonstrate that this detector has substantial electron background rejection capability (greater than 99.8%) and can utilize various target nuclei, such as hydrogen and argon.

PACS numbers: 95.55.Vj, 29.40.Cs, 95.35.+d

One of the most compelling questions of modern physics is the existence and nature of dark matter (DM) in the Universe. There is considerable observational evidence [1] that as much as 90% of the matter in the cosmos does not interact electromagnetically and betrays its existence only through gravitational effects. Spiral galaxy rotation curves imply a DM component which is present on galactic scales. One popular model explaining the flatness of galactic rotation curves postulates the existence of a self-gravitating, isothermal, spherical distribution of weakly interacting massive particles (WIMPs). The distribution of particles is assumed to be nonrotating and is supported against gravitational collapse by the random thermal velocities of the particles. The canonical models assume a simple Maxwellian velocity distribution ($\bar{v} \sim 300$ km/s) with a cutoff at the galactic escape velocity.

Extensions to the standard model provide many particle DM possibilities with supersymmetry (SUSY) contributing one of the most promising candidates, the neutralino ($\tilde{\chi}$). The mass and couplings of the $\tilde{\chi}$ depend upon several parameters in the theory, but once specified, cross sections for interaction with ordinary matter [2] can be calculated. Typical cross sections for elastic scattering on nuclei are $\sigma \sim 10^{-38}$–10^{-36} cm^2 and masses range from 1 to 1000 GeV.

The Earth's motion through the galactic halo can provide distinctive signatures for WIMP detection. The average velocity of the Earth through the halo is the circular velocity $v_\odot \approx 220$ km/s of the Sun around the galactic center. Simple two-body kinematics with terrestial nuclei give maximum recoil energies in the keV region. Assuming knowledge of the local mass density of WIMPs in the halo (~ 0.3 GeV/cm^3), it is possible to estimate [3] the interaction rates of weak elastic scattering to be $\sim 0.01 - 1000$ events/(kg day), depending upon WIMP mass, σ, and the detector used.

In the past several years there have been a number of experiments and proposals [4] for detecting WIMPs. Most direct searches rely upon the elastic scattering of WIMPs with ordinary matter producing a recoiling nucleus which is detected by measuring its kinetic energy. The earliest experiments using Ge [5] and Si [6] crystals were able to rule out some DM candidates such as Dirac neutrinos and cosmions with cross sections the order of 10^{-35} cm^2. These types of experiments are ultimately limited by photon induced backgrounds from Compton scattering and the photoelectric effect. Recent work on cryogenic Ge [7] and Si [8] crystals demonstrates enhanced background rejection by use of simultaneous measurements of thermal phonons and ionization signals to distinguish between electron and nuclear recoils. Discrimination ideas based on crystal or liquid noble gas scintillators [9] have also been suggested.

Ultimately, a positive identification of a WIMP signal will probably require more than just a measurement of the recoil energy. Drukier, Freese, and Spergel [10] have shown that the varying component of the Earth's velocity around the Sun produces a yearly modulation in the number of recoil events depositing energy above a fixed detector threshold. Because the rate varies by only 5%–10% over the course of a year, this seasonal modulation can provide a unique signature only if a significant number of events are observed.

A much more powerful method for distinguishing signal from background is to measure not only the nuclear recoil energy, but also its direction. Spergel [11] has considered the case of an isothermal halo of WIMPs (mass m_x), and shown that the rate of events in which the nucleus (mass m_N) recoils with energy E into a cone of opening angle γ with respect to $-\vec{v}_\odot$ has the form

$$\frac{dR}{dE\, d\cos\gamma} \propto \exp\left[\frac{-[v_\odot \cos\gamma - v_{\min}]^2}{v_{\text{halo}}^2}\right], \qquad (1)$$

where $v_{\min}^2 = (m_N + m_x)^2 E/2m_N m_x^2$ is the minimum WIMP velocity that can produce a nuclear recoil of energy E, and $v_{\text{halo}}^2 = 3v_\odot^2/2$. The expression above shows that the nuclear recoil direction has a strong angular dependence, which can be exploited to distinguish between signal (WIMP induced nuclear recoils) and background. Depending upon the detector velocity threshold,

this gives very large ratios (4–30) for the recoil direction asymmetry (ratio of forward to backward recoils with respect to $-\vec{v}_{\odot}$). A detector operated on the surface of the Earth will experience a 24 h period variation in the orientation of the detector coordinate system relative to the direction of motion through the galactic halo (given by $\vec{v}_{\odot}$). Hence, the average target recoil direction (as reconstructed in the detector coordinate system) will experience a diurnal variation. It should be noted that the expected background events (neutrons, Compton electrons, etc.) present in the detector, could, in principle, show a similar asymmetry in a preferred direction (in the detector system). However, the possible background asymmetry is expected to be independent of time. The recoil direction asymmetry and the associated diurnal modulation demonstrates the utility of a detector system capable of resolving the actual direction (or projected direction) of nuclear recoils.

The detection scheme described here differs significantly from all others in that it uses a rarified gas as the target material. The pressure of the gas is reduced to levels that extend the range of nuclear recoils (5–50 mm) which can then be detected and reconstructed by using conventional gas detector techniques. Thus, the recoil direction as well as energy is obtained. A second important feature of this detector is its ability to separate a WIMP induced nuclear recoil from the photon induced backgrounds (Compton and photoelectrons). The detector operates in a 4.5 kG magnetic field, which yields a radius of curvature of 1 mm for an electron of 10 keV. As the electron loses energy in the gas and spirals inward, multiple scattering and the limited resolution of the detector system will tend to alter the track structure, but circular symmetry is maintained and an intense central core of ionization develops. Thus, the photon induced electrons will appear as roughly circular, distinct structures. In comparison, nuclei have a much larger radius of curvature (> 10 cm) and therefore appear as elongated structures.

The prototype detector described here has evolved from earlier work [12] on low pressure time projection chambers (TPCs) using conventional multiwire readout techniques. This new device (refer to Fig. 1) consists of an optically imaged multistage parallel plate avalanche chamber (PPAC) coupled to a large detection volume, containing 100 L of a proportional gas with an additive of triethylamine (TEA) vapor at 7% partial pressure. Two different gas mixtures have been tested. When filled with CH_4 at 20 torr the detector contains 0.56 g of hydrogen targets. A P-10 gas mixture (90% Ar and 10% CH_4) at 50 torr with Ar as the primary target nucleus provides 9.8 g of detector mass.

The detection volume is contained within a stainless steel cylinder of 40 cm diameter and 1 m in length. It is bordered on the end caps by a high voltage plate and the first (ground) screen of the PPAC, and the inner surface of the cylinder is lined with a field cage consisting of a series of copper rings. The combination of end cap electrodes and field cage provide a uniform electric field throughout the detection volume. Primary ionization tracks formed in the gas by the passage of charged particles are drifted in this field to the PPAC detector end cap. In transporting the primary ionization through the drift region to the sense plane, both transverse and longitudinal diffusion will distort the track. A localized source of electrons drifted a length, z, of the detector volume will spread to form a Gaussian spatial distribution of width $\sigma_t \propto \sqrt{z}$ in the x-y plane. In order to suppress this transverse diffusion, the entire detection volume is contained within a warm-bore superconducting magnet with a field of 4.5 kG oriented in the direction of the electric field. After drifting a distance of 1 m in 20 torr of CH_4, we have measured [13] $\sigma_t < 1$ mm which exceeds the resolution of the imaging system ($\sigma_t \simeq 15$ mm with no magnetic field). The longitudinal diffusion is unaffected by the presence of a magnetic field, and remains quite large at reduced pressures. For this reason, no timing information is used, and only a two-dimensional projection of charged particle tracks is obtained subsequent to the drift.

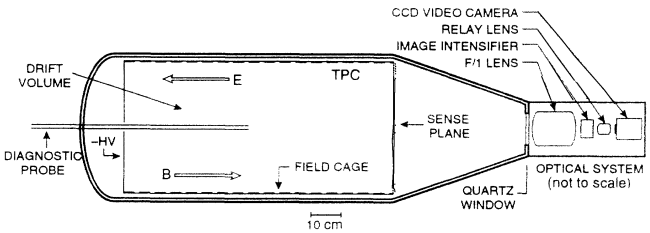

FIG. 1. A schematic view of the low pressure TPC and optical system.

The sense plane consists of two standard PPAC detectors of gap width 6.4 mm sharing a common screen between them. In order to achieve higher gains [14], a transfer region is usually inserted between the two stages of the device. In testing various detector configurations, we have determined that the resulting increase in gain is achieved at the expense of spatial resolution, and thus, in the present design no transfer region was used. It is well known that photons are copiously produced [15] in the charge amplification process. The addition of TEA molecules to the gas mixture greatly enhances the photon yield, producing a dominant UV component ($\bar{\lambda} \sim 280$ nm) which can be imaged with specialized optics through the detector screens. The total charge gain in the device (10^5–10^6) is accompanied by a photon yield [16] of about 1 photon per electron in the avalanche. The light produced by the avalanche process is proportional to the initial or primary ionization deposited in the detector gas. Hence, imaging the PPAC chamber yields a two-dimensional projection of particle tracks, as well as a measure of the energy loss, dE/dx, along the track.

The light generated in the PPAC is imaged by a UV

grade $f/1$ lens onto the photosensitive surface of an image intensifier tube. The output of the intensifier displays the demagnified image on a phosphor screen ($\lambda \approx 550$ nm), and an $f/2$ 1:1 relay lens transfers the image onto the surface of a 512 by 512 charge coupled device (CCD) array. The ratio of photons arriving at the surface of the CCD to the number of photons produced in the avalanche is approximately 4×10^{-3}. Images thus obtained are transferred to the computer, and can be filtered, displayed, or stored to disk for subsequent analysis.

Several tests have been made with radioactive sources to evaluate the performance of the detector. In addition to establishing the minimum observable track length, we are primarily interested in determining the level of photon background rejection, and in obtaining an energy calibration for the detector. In these measurements, gas mixtures of CH_4/TEA and P-10/TEA were both used. A Cf ^{252} source provides neutrons which elastically scatter from the target gases producing ion recoils (mostly H and Ar) with energies of a few keV to several MeV. Accompanying the neutrons are gamma rays also covering the same energy range. Figure 2 is a CCD image showing an example of the images obtained by exposing the detector (with P-10) to the neutron source. The image contains both ion recoils (tracks) and circular patterns of electrons resulting from gamma scattering. The electron events fall into two distinct categories. First, the extended "ring" structure which is dimly present, is consistent with a minimum ionizing (~MeV) electron which follows a helical path down the bore of the detection volume. The ring represents the projection of the helix on the detector plane. Such high energy electron events are easily distinguished due to low ionization along the trajectory and their unique annular shape. However, the low energy electrons give a higher ionization density due to a larger dE/dx and a lower radius of curvature as they "range out" in the gas. In most cases, the resulting circular electron pattern is easily distinguished from the ion recoils. A topological parameter ϵ (similar to eccentricity) can be defined as $\epsilon^2 = 1 - \lambda_-/\lambda_+$, where the $\lambda_\pm$ represent the second moments of the light distribution along the principal axes. This parameter can be used to quantitatively separate electrons (symmetrical structures) from ion recoils (track structures). Figure 3 shows a histogram of ϵ^2 values obtained from pure electron data (^{57}Co source with x-ray energies of 6.5 keV and 14.4 keV). A preliminary cut at $\epsilon^2 = 0.37$ yields a 99.8% rejection of the electron events. This rejection level is independent of energy down to at least 6 keV. Also displayed in Fig. 3 is a histogram of the ^{252}Cf neutron source data which clearly shows an electron contamination peak at small ϵ^2, as well as an extended tail in the distribution caused by the nuclear recoil tracks. If we assume that the nuclear recoil distribution extends at the same level under the electron peak, the cut at $\epsilon^2 = 0.37$ would remove $\sim 25\%$ of the nuclear recoils.

The detector can be directly calibrated in terms of energy by observing the electron structures produced by the 6.5 and 14.4 keV x rays of the ^{57}Co source, and a histogram of the total amount of light contained in such structures clearly shows two distinct peaks corresponding to these energies. However, the useful detection threshold is given by a minimum projected track length of 5 mm (corresponding to the cut in epsilon mentioned earlier). A total range of 5 mm in 20 torr of CH_4 corresponds to a hydrogen ion energy [17] of 2 keV, while the same range in 50 torr of P-10 corresponds to an argon ion energy [18] of 8 keV.

A Monte Carlo simulation of the detector system, which includes recoil kinematics, the orientation of the detector on the Earth, the Earth's rotation, and a cut-

FIG. 2. A false color CCD image resulting from a ^{252}Cf neutron source. The colors black, blue, red, and white represent the order of increasing light intensity levels. The area displayed represents a 25 cm by 25 cm section of the detector plane. See the text for a description of image features.

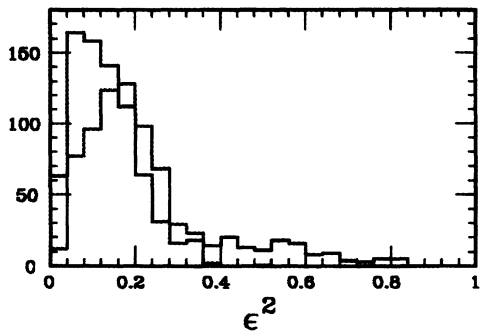

FIG. 3. Histogram of topological parameter ϵ^2 (defined in text). The dashed line corresponds to the ^{57}Co (electron) data, and the solid line corresponds to the ^{252}Cf (electron and nuclear recoil) data.

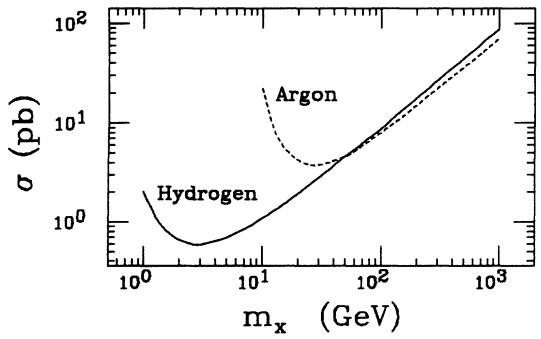

FIG. 4. Exclusion plot of cross section $\sigma(\tilde{\chi}N \rightarrow \tilde{\chi}N)$ versus neutralino mass for both hydrogen (solid line) and argon (dotted line) targets obtained by Monte Carlo simulation (see text for details). The region above the curves would be excluded after running the prototype for 1 yr live time if no events are found.

off in projected (identifiable) track lengths of 5 mm, has been used to determine the efficiency of detecting nuclear recoils above a given energy threshold. Random recoil energies and directions were generated from Eq. (1), and the projected track lengths as seen in the detector plane were found. In the region where $m_x \gg m_N$, the recoil detection efficiency has been determined to be 70% with an energy threshold of 2 keV for hydrogen in 20 torr of CH_4, and 92% for an 8 keV threshold for argon in 50 torr of P-10. (It should be noted that the recoil detection efficiency quoted does not include the relative ionization efficiency, which can be predicted from the Linhard model and measured directly with neutron scattering experiments. Also, the efficiency quoted for Ar in P-10 does not take coherence losses into consideration.)

Figure 4 shows the resulting possible exclusion plots of cross section versus WIMP mass, in which the region above the curves would be excluded at the 95% confidence level if no events are seen at the end of 1 yr live time. At $m_x \gg m_N$, the rates corresponding to the cross section limits are 50 events/(kg day) for hydrogen and 1 event/(kg day) for argon. The usual assumptions on halo density and velocity have been made. A theoretical calculation of event rates [2] shows that the cross section is expected to be somewhat lower than these limits, however, a significant amount of parameter space can still be eliminated if background can be sufficiently suppressed.

The CCD imaged PPAC operating at reduced pressure has been shown to be a potentially powerful device for the detection of WIMPs in the galactic halo. Recoiling nuclei in the proper energy region have been successfully imaged and clearly distinguished from electron background signals at the level of a few parts per thousand. This technique gives the nuclear recoil direction as well as the energy. The ability to measure the diurnal modulation in the average nuclear recoil direction (absent for background sources) provides a positive signature for WIMP interactions which is not achievable by most other techniques.

We are extremely grateful to K. Griest for useful discussions, and to P. Smith for pointing out an error in the original manuscript. The authors also wish to acknowledge A. Breskin, G. Charpak, and F. Sauli for enlightening correspondence.

[1] V. Trimble, Annu. Rev. Astron. Astrophys. **25**, 425–472 (1987).
[2] K. Griest, Phys. Rev. D **38**, 2357 (1988).
[3] M.W. Goodman and E. Witten, Phys. Rev. D **31**, 3059 (1985).
[4] J.R. Primack, D. Seckel, and B. Sadoulet, Annu. Rev. Nucl. Part. Sci. **38**, 751 (1988); P.F. Smith and J.D. Lewin, Phys. Rep. **187**, 203 (1990).
[5] D.O. Caldwell *et al.*, Phys. Rev. Lett. **61**, 510 (1988); S.P. Ahlen *et al.*, Phys. Lett. B **195**, 603 (1987).
[6] D.O. Caldwell *et al.*, Phys. Rev. Lett. **65**, 1305 (1990).
[7] T. Shutt *et al.*, Phys. Rev. Lett. **69**, 3425 (1992).
[8] N.J.C. Spooner *et al.*, Phys. Lett. B **273**, 333 (1991).
[9] P.F. Smith and J.D. Lewin, Philos. Trans. R. Soc. London A **346**, 111 (1994).
[10] A.K. Drukier, K. Freese, and D.N. Spergel, Phys. Rev. D **33**, 3495 (1986).
[11] D. Spergel, Phys. Rev. D **37**, 1353 (1988).
[12] G. Masek, K. Buckland, and M. Mojaver, in *Proceedings of the Workshop on Particle Astrophysics, 8–10 December 1988*, edited by E. Norman (World Scientific, Singapore, 1989); G. Gerbier, J. Rich, M. Spiro, and C. Tao, *ibid.*
[13] K.N. Buckland, G.E. Masek, M.J. Lehner, and M. Mojaver (to be published).
[14] A. Breskin, R. Chechik, and D. Sauvage, Nucl. Instrum. Methods Phys. Res., Sect. A **286**, 251 (1990).
[15] G. Charpak *et al.*, IEEE Trans. Nucl. Sci. **35**, 483 (1988).
[16] G. Charpak *et al.*, Nucl. Instrum. Methods Phys. Res., Sect. A **269**, 142 (1988).
[17] H. Andersen and J. Ziegler, *The Stopping and Ranges of Ions in Matter Vol. 3* (Pergamon Press, New York, 1977).
[18] A. Fukuda, J. Phys. B **14**, 4533 (1981).

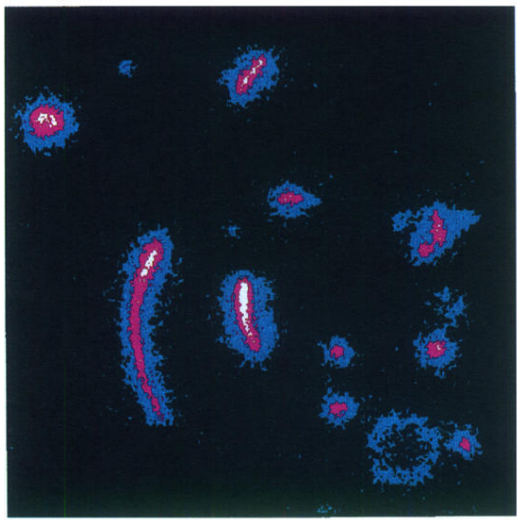

FIG. 2. A false color CCD image resulting from a ^{252}Cf neutron source. The colors black, blue, red, and white represent the order of increasing light intensity levels. The area displayed represents a 25 cm by 25 cm section of the detector plane. See the text for a description of image features.

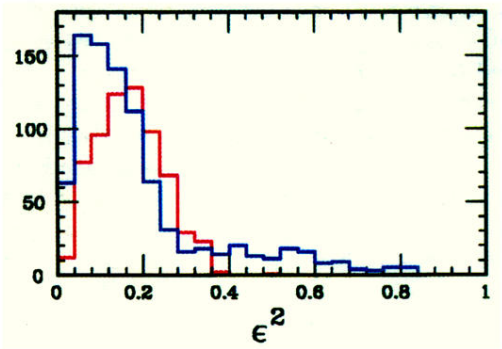

FIG. 3. Histogram of topological parameter ϵ^2 (defined in text). The dashed line corresponds to the ^{57}Co (electron) data, and the solid line corresponds to the ^{252}Cf (electron and nuclear recoil) data.